Zwitterionic Osmolytes Employ Dual Mechanisms for Resurrection of Surface Charge under Salt-stress

Susmita Sarkar, Anku Guha, T. N. Narayanan, and Jagannath Mondal*

Tata Institute of Fundamental Research, Center for Interdisciplinary sciences, Hyderabad 500046, India

E-mail: jmondal@tifrh.res.in,+914020203091

Abstract

Salt imbalance in cells is a major detrimental abiotic stress which causes ionic toxicity and disrupts important cellular functions. To counter this saline stress, cell often produces low molecular weight cosolutes, known as osmolytes, which have the ability to resuscitate homeostasis. Here we combine atomistic computer simulation, contact angle measurements and Raman spectroscopic analysis to identify the mechanistic role of multiple osmolytes (glycine, TMAO and betaine) in modulating the electrostatic interaction under salt stress, a slowly emerging aspect of osmoprotection. By utilising a pair of negatively charged silica surfaces in a ternary mixture of osmolyte and KCl solution as a proxy of charged surface of biomacromolecule, our investigation reveals that all three osmolytes are able to resurrect the electrostatic interaction between the two surfaces, which had been otherwise charge-screened by excess salt. The joint venture of experiment and simulation discover dual and mutually exclusive mechanisms of recovering charge interaction by zwitter-ionic osmolytes. However, the relative ability and the underlying mechanism of revival of electrostatic interactions are found to

be strongly dependent of chemical nature of osmolyte. Specifically, glycine was found to competitively desorb the salt-ions from the surface via its direct interaction with the surface. On the other hand, TMAO and betaine counter-act salt stress by retaining adsorbed cations but partially neutralising their charge-density via ion-mediated interaction. We believe that the access to dual and mutually alternative modes of osmolytic actions, as elucidated here, would provide the cell the required adaptability in combating salt-stress.

Significance statement

Osmolytes protect cell-life from salt-stress and restore cellular functions. Combined computational (atomistic computer simulation) and experimental (contact angle, Raman spectroscopic analysis) effort, characterizes the mechanistic role of different osmolytes (glycine, TMAO and betaine) in modulating Coulombic interaction. This investigation uncovers dual and mutually independent mechanisms (driven by chemical nature of zwitter-ionic osmolytes) of restoring electrostatic interaction among two surfaces, which was charge-screened during salt-stress. Glycine directly interacts with surface to desorb the salt-ions whereas TMAO and betaine while retaining cations, partially neutralise their charge-density to counter salt-stress. This mechanistic insight of osmolytic performance helps in effective drug-designing. Moreover these dual and mutually contrasting osmolyte interactions, would itself assist cells for being more adaptable and flexible towards adverse changes of nature.

Introduction

The cellular interior is constituted of large number of biomacromolecules with negatively charged surface groups (for example, in the form of nucleotides and amino acid carboxylates), which are balanced by positively charged residues and inorganic salts involving K^+ and Mg^{+2}. While a low concentration of salt is required to preserve the biological activities[1,2]

and the fold of the macromolecules inside the cell,[3] excess concentration of salts is frequently held responsible for cellular dysfunctions. Almost all the organisms suffer from tremendous osmotic shock[4] and their respective bio-actions are inhibited due to drastic change of osmolarity[5,6] of the surroundings as in saline soil, marine water and renal fluids etc. Specifically, saline stress has been considered as the most severe abiotic stress to harm wide range of organisms in great extent. As a part of resistance mechanism, a series of small zwitterionic organic molecules, known as osmolytes, are often produced by cells which have the ability to stabilize biomolecular structures and prevent biological instability.[1] Along with the primary osmoregulation, osmolytes encounter several detrimental effects evolved from salt stress. There are multiple osmolytes (proline, betaine, glycine, trimethylamine N-oxide etc) known to maintain biomolecular solubility under excess salt concentration and maintains proper cellular functions.[1,2] Protection of macromolecular stability[7] during salt-stress is also guided by several osmolytes.

Traditionally salt-stress encountering ability by osmolytes is believed to be governed by their stabilizing or dis-stabilizing effect on bio-macromolecules.[8–12] Osmolytic influence has routinely been practised based on non-coulombic force and water mediated interactions.[13] But the interactions of osmolytes with the biomolecular surfaces, in particular how these molecules modulate the surface charge density and electrostatics, has eluded mainstream investigations. However the abundance of negatively charged macromolecules in the cellular interior warrants detailed investigation on how osmolytes would counteract the potential saline stress faced by these negatively charged species. Recent investigation by Pielak and coworkers revealed Coulombic influence of osmolytes responsible for maintaining osmotic balance.[3] Again another current investigation by Govrin et al.[14] also add more on this trend. As a proxy to negatively charged surfaces of biomacromolecule, Govrin et al.[14] examined the influence of salt on the electrostatic interaction of two negatively charged silica surfaces and found that salts are prone to screen the surface charge and destabilise the system by reducing inter-plate repulsion. Their investigation explored the combined effect of salts and osmolytes

on negatively charged silica plates via atomic force microscopy (AFM). The osmolytes were found to counteract the screening effect of salts and revive their electrostatic repulsion and a competitive osmolyte-induced desorption mechanism was hypothesised. However the underlying mechanism has not been elucidated in specific molecular details.

In this present investigation, we have revisited the question of molecular mechanism of osmolyte activity against salt-stress, via a combination of atomic-resolution simulation and experimental measurements. Here we have employed a pair of parallel silica plates to investigate the individual and combined roles of salt (KCl) and a set of osmolytes (glycine or TMAO or betaine) in modulating the inter-plate electrostatic interaction via computer simulation. While our simulations recapitulate the recent experimental trends[14] on impact of osmolytes on inter-plate interaction in saline medium, we discover that the modes of all of these osmolytes' actions are not same for all. Our investigation identifies that there are, in fact, dual mechanism for restoring salt-screened electrostatic interactions by osmolytes that are at play and the mechanisms are highly sensitive to the nature of chemical structure of the osmolyte molecules. Depending on the divergent zwitter-ionic nature of the osmolytes, some of them are found to competitively desorb cations, while for others, the phenomenon of cation neutralization induced by osmolytes act as the core interaction in counteracting salt-stress. We validate our proposed mechanism via contact angle measurements and Raman spectral analysis.

Materials and methods

The investigation described in current article involves a combined venture of atomistic resolution modelling and adsorption experiments. Below we describe each of them individually:

Simulation model: In this project we aim to figure out the biological functions of osmolytes upon osmotic stress and hence we have considered two negatively charged silica plates as our system of interest. Since the biological entities are generally accompanied with

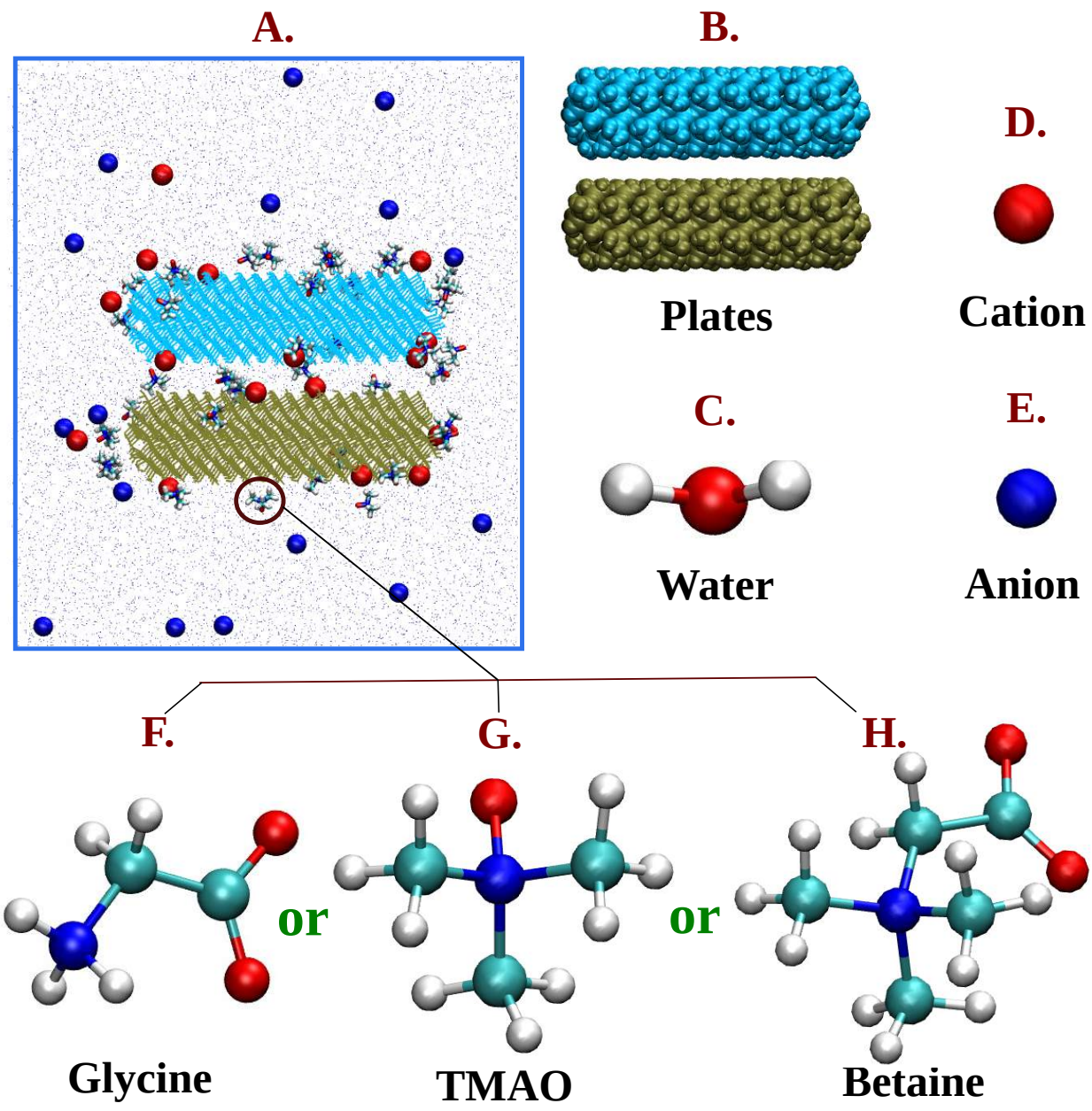

Figure 1: A. The representation of the simulation system. B. two parallel silica plates with negative charge (shown in cyan and olive green color). C. the water molecule. D-E. are showing cation and anion in red and blue coloration respectively. Representative structures of osmolyte molecules, glycine, TMAO and betaine are also shown in figure F, G and H respectively. Red, blue, cyan and white colors are representing Oxygen, Nitrogen, Carbon and Hydrogen atoms respectively.

multitudes of negatively charged species (mostly nucleic acid phosphates and amino acid carboxylates), Govrin et al[14] have recently utilised a pair of negatively charged silica surfaces as a suitable proxy to investigate the role of osmolytes in a saline medium in a series of recent investigations. Silica, an well-known inorganic protic surface, has been utilised as good model systems in recent experiments[14–16] because it recapitulates many of the properties exhibited by negatively charged proteins, without the inherent complications brought out with protein structure. In both cases the surface acquires its negative charge by deprotonation of weak acids, carboxyl ones in the case of proteins and silanols in the case of silica. Inspired by these previous investigations, a set of nanoscale-sized model silica surface forms the base of current modelling investigation. Here we have employed *nanomaterial builder* module[17] of CHARMM-GUI server[18] to generate the desired silica surface in the form of a cuboid box of silica (α-Quartz (SiO_2)) with dimension X: 4 nm, Y: 4 nm and Z: 1 nm and Miller Index 0,0,1. Silanols, on the surface of the silica plate, become deprotonated partially to give rise to a pH-dependent negative surface in contact with the aqueous solution. To investigate the effect of extent of charge, we have modelled these two plates at a given pH 5.6 . Towards this end, the charge on the surface of silica plates was tuned by modifying the relative proportion of Si-OH and SiO^-Na^+ on the silica surface, commensurate with a given pH, which decides its degree of ionization. In particular, at pH 5.6 the degree of ionization was maintained at 7.4 %. For checking the robustness of our results, we have also carried out additional simulation at pH 8.0, at which the degree of ionization was 16.6 % . As a benchmark, we first simulate the interaction between the surface pairs in neat water and in aqueous salt solution at range of concentrations (0.50 mM to 2 M potassium chloride (KCl) solution). As the main part of the investigation in this work, we have compared the effect of three osmolytes, namely glycine, TMAO and betaine on interaction between two silica surfaces. The individual effect of osmolyte and also combined effect of each of the three osmolytes (1.5 M) in presence of 50 mM KCl salt are mainly analysed. Table 2 provides the details of all systems employed in the current investigation. A periodic box of dimension of 8×8×10

nm^3 has been employed in each of the systems investigated here. The Silica surfaces have been modelled via interface force field.[19–22] The inorganic ions in salt have been modelled via Charmm force field[23] and the osmolytes parameters are employed from a previous report of Mukherjee et al.[24–29] In our simulation we have used charmm-TIP3P model[30] to model water.

Simulation Method:

In the current study we have employed classical molecular dynamics (MD) simulation to investigate the interaction of a pair of negatively charged silica plates, in aqueous saline medium in presence as well as in absence of a set of osmolyte molecules (see figure 2). To quantify the extent of interactions between the two plates, we compute the mean force between these two silica plates, placed mutually parallel with each other, in each of the aqueous media employed in this work. We repeat the process by scanning the inter-plate distances from 1.5 nm to 2.0 nm with a spacing of 0.02 nm, keeping the relative tilt angle between the plates to zero degree. The procedure results in a force profile as a function of inter-plate distance.

Prior to force calculation corresponding to a given inter-plate separation, the system is first subjected to a step-wise protocol of equilibration. Towards this end, the system is initially energy minimised with steepest-descent algorithm and then subjected to a very short NPT equilibration of 50 ps at 298.15 K average temperature and at equilibrium pressure of 1 bar. During simulation the temperature and pressure are maintained using velocity rescale thermostat[31] and with Berendsen barostat[32] respectively. Subsequently we have proceeded for final production run in NVT ensemble with the NPT equilibrated system. During NVT production run we have kept the system temperature fixed as same as before i.e. 298.15 K and we have employed Nose-Hoover thermostat[33,34] (time constant $\tau_T = 1.0$ ps) to maintain the temperature. A leap-frog integrator with a time step of 2 femtosecond was employed for time propagation. 1.2 nm cut-off has been chosen in case of van der Waals and Coulomb interaction. For treatment of long-range electrostatic interactions particle-

Mesh Ewald (PME)[35] method has been employed. In our simulation to constrain the bonds associated with hydrogen and for bonds as well as angle of water molecules, LINCS[36] and SETTLE[37] algorithms respectively are employed. 2018.6 version of GROMACS software[38] are used to execute all the molecular dynamics (MD) simulations. Throughout all stages of simulations, the plates were kept fixed at their desired position by using 'freeze group' utility within GROMACS. The forces were time-averaged over the last 15 ns of each of the production runs to obtain the mean force between two plates. To assess the mechanism of salt action we have focussed on two inter-plate separations at 1.6 and 1.8 nm. At these two separations, we have carried out simulations for relatively longer time (50 ns each) and each simulations are replicated five times following the aforementioned simulation protocol. Identical protocol was employed for each of the systems investigated in the current work.

To characterise the underlying mechanism, we have calculated density profile and also estimated pair correlation function. For evaluating the interaction of plates with salt-cation or osmolytes and also osmolytic interaction with K^+ ions adsorbed to the surface we have calculated pair correlation function of both the parts of the zwitter-ionic parts (negatively and positively) of the osmolytes with respect to either K^+ ions or the silica plates. Since the two ends of the zwitterions are capable of two exactly opposite modes of electrostatic interaction, estimation of interaction for each of the part of the osmolyte molecule would provide the clear view about the mechanism. To assess the binding affinity of different species we have introduced preferential binding coefficient (Γ_s)[39,40] calculation. This quantity will provide us with the idea of how different entities (cation of a salt, K^+ here and both the parts of zwitter-ionic osmolyte) are interacting with the silica plates. Γ_s can be expressed as

$$\Gamma_s = \left\langle n_s - \frac{N_s^{tot} - n_s}{N_w^{tot} - n_w} \cdot n_w \right\rangle \tag{1}$$

where n_s represents the number of species (either salt cation or osmolytic part) bound to the silica surface, ${N_s}^{tot}$ is the total number of species present in the entire system, n_w stands

System	Number of K^+ /Cl^- ions	Number of glycine/TMAO/betaine molecules	Number of water molecules	Concentration
KCl	0 16 32 64	0 0 0 0	19313 19254 19235 19162	0 M 50 mM 1 M 2 M
Glycine in 50 mM KCl	16	579	16847	1.5 M
TMAO in 50 mM KCl	16	579	16256	1.5 M
Betaine in 50 mM KCl	16 16 16 16	386 579 772 1158	16601 15202 13924 11325	1 M 1.5 M 2 M 3 M
Betaine in 0 mM KCl	0	579	15174	1.5 M

Figure 2: The details of the simulation systems used for computational study at pH 5.6 are represented in tabular form. All the simulations are done in presence of a pair of negatively charged silica plates and the negative charge of the system is neutralized by sodium ions (62 Na^+ ions). KCl salt and osmolyte (glycine: gly, TMAO: tma and betaine: bet) concentrations employed in each of the system are indicated with clear details of the number of salt ions, osmolyte molecules and water (w) molecules shown in respective brackets.

for the number of water molecules which are bound to the surface of silica plate, and ${N_w}^{tot}$ is the total number of water molecules of the system. The measure of the excess of that species (referred as 's') around silica surface is quantitatively represented by Γ_s in comparison to its average concentration in the solution. To determine preferential interaction of osmolytes with silica plates, two opposite parts i.e anionic and cationic parts of the osmolytes are taken into account for calculation of Γ_s by considering zwitter-ionic nature of osmolytes. A positive value of Γ_s would provide a measure of favourable preferential binding of the species under consideration, to the silica surface, whereas $\Gamma_s < 0$ indicates the depletion of that entity from the surface of silica.

To validate the predictions from simulation, a set of experimental investigations were undertaken. In particular, contact angle and spectroscopic measurements are performed as described below.

Experimental material and methods

Materials: We have measured contact angle and also analysed the Raman spectral changes due to the influence of salt and osmolyte interaction with the silica surface. For those measurements we have used Potassium chloride (KCl), glycine, TMAO (trimethylamine N-oxide), betaine, acetic acid, and sodium acetate all of which are bought from sigma Aldrich and used without further purification. Type-I DI water is used for preparing the solutions of salt and different osmolytes of variable concentration. We have used one side polished silicon wafer with native oxide layer which is bought from micro-chemicals.

Contact angle measurements:

All the room temperate contact angle measurements are performed using VCA optima instrument. Thoroughly cleaned syringe is used for the measurements. The silica wafer (silicon wafer having native oxide) is cleaned by IPA and is dried with an air blower. The experiments are performed several times and the measurement error is tabulated.

Synthesis of Au np core-SiO_2 shell (Au@SiO_2 np) nanoparticle:

SiO_2 coated Au nanoparticle (55 nm) were synthesised using a method reported elsewhere.[41,42] Initially, 200 mL 0.01 wt% $HAuCl_4$ was boiled at 140°C and then 1.4 ml 1 wt% Sodium citrate was added to synthesise Au np (55nm) which was stored in refrigerator. 30 ml as prepared sample was mixed with 0.4 ml 1mM (3-aminopropyl)triethoxysilane (APTES) and then 0.54 wt% 3.2 mL of sodium silicate with a pH of ∼10 was added to the solution. Then the mixture was transferred to 95 °C bath and stirred for 30 mins. As prepared SiO_2 coated Au np was centrifuged twice and washed with DI water and concentrated solution was kept in refrigerator. The concentrated solution was diluted and dropcasted on cleaned Si substrate with native oxide before the SHINERS[42] experiments.

Micro Raman analysis: All the Surface enhanced Raman spectra (SHINERS)[42] are taken using a micro-Raman spectrometer (Renishaw In-via Spectrometer) on a Au np core (55 nm)-SiO_2 (5 nm) shell dropcasted silicon with native oxide having the different osmolytes in acetate buffer containing 50 mM KCl with 532 nm laser excitation using L5x lens. The time for recording data is optimized to 10 sec using 50% laser power for a better signal-to-noise ratio. Schematic of the SHINERS experimental set is illustrated in figure 3.

Results and Discussion

Osmolytes counteract salt stress.

We started our investigation by measuring the value of force between the two negatively charged silica surfaces in neat water as a function of inter-plate separation. As depicted in figure 4A, the present model correctly reproduces a repulsive force profile, as would be expected from electrostatic repulsion between two plates of like charge. To assess the individual role of salt, we computed the force curve between these two surfaces solvated in 50 mM aqueous KCl solution. A quantitative comparison of the force profiles (figure 4A) confirmed that the force experienced by the two plates is considerably reduced in the saline media (red curve, figure 4A) than that in neat water (blue curve, figure 4A). The reduction

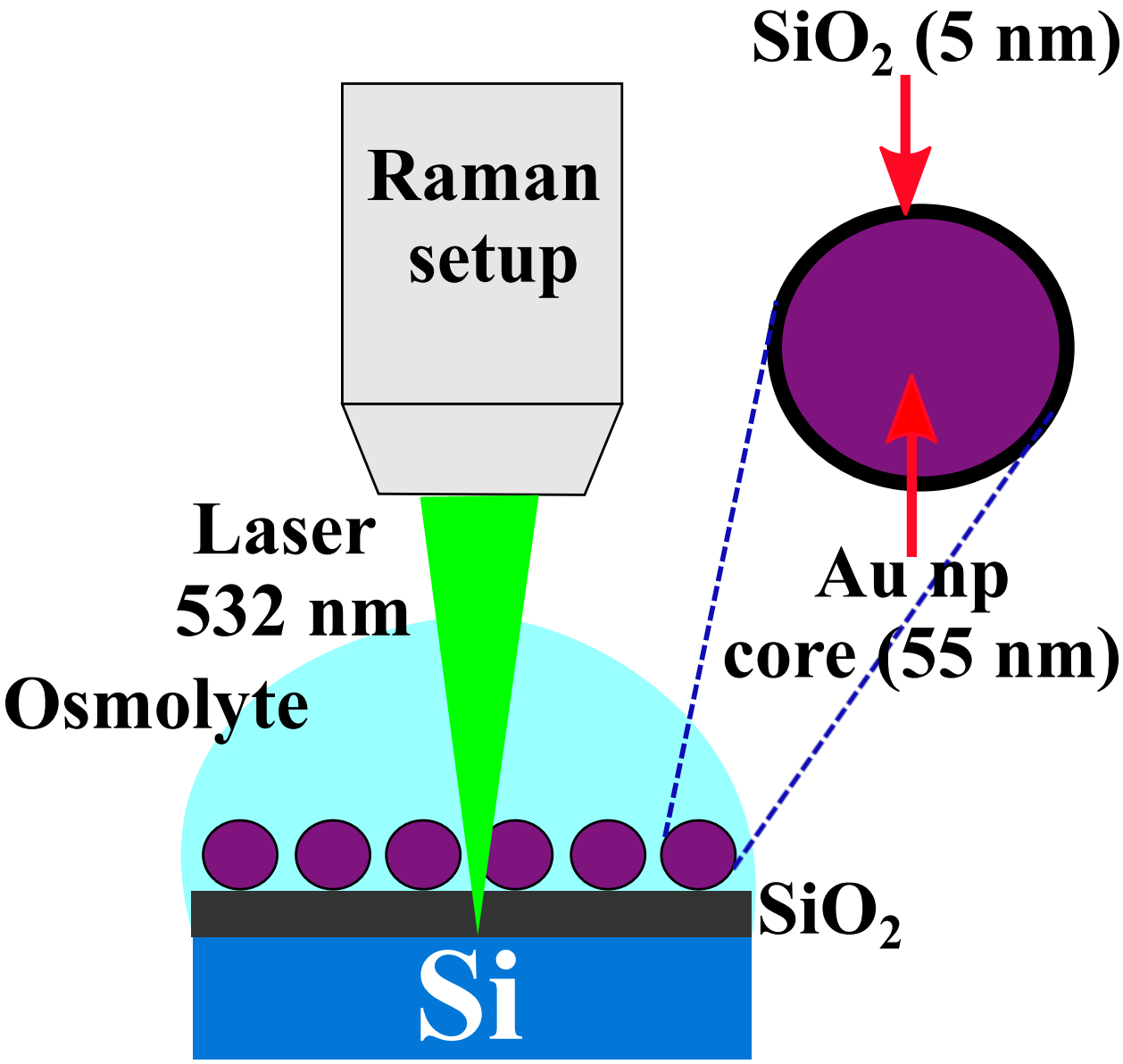

Figure 3: A schematic of experimental set up of Surface enhanced Raman spectra (SHINERS) is shown in this figure.

of the inter-plate force follows a monotonic trend upon gradual increase of salt concentration ranging between 50 mM to 2 M (see figure S1 A). The screening of plate charges due to adsorption of cation (K^+ ions) is traditionally well-proven mechanism for reduction of repulsive force, which is also at play here, as reflected by the sharp rise in density profile of cations around the plates compared to the bulk solution (figure 5A). This result is a prototypical recapitulation of salt-stress which is known to induce risky biomolecular aggregation and protein instability by favouring abnormal protein-protein communication in high-salt environment.

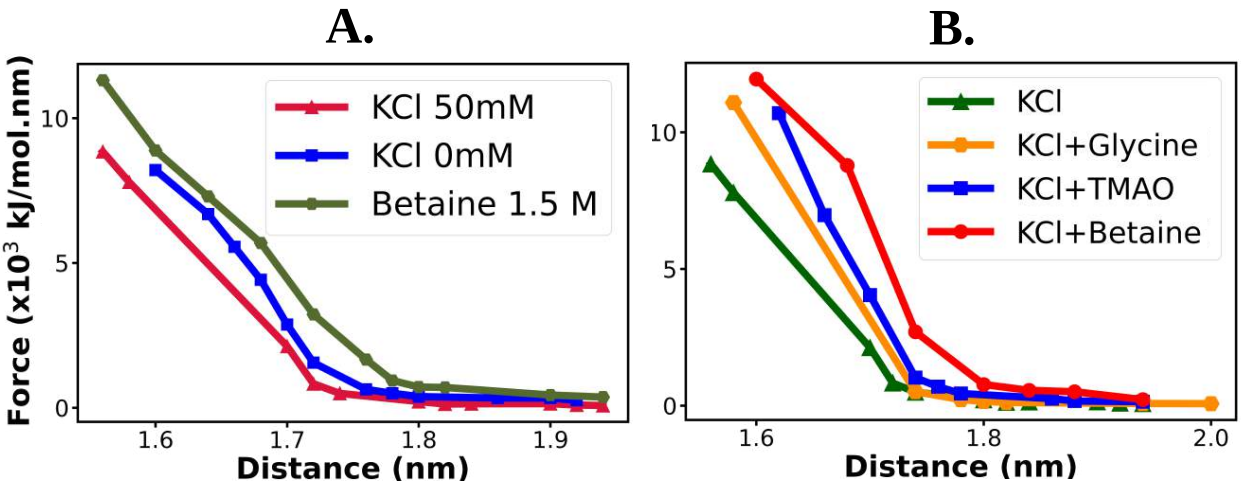

Figure 4: Influence of additives on force experiencing between two negatively charged silica plates, represented by the plots of distance profile of force of silica plates A. in neat water, 50 mM KCl and 1.5 M osmolyte (Betaine) in absence of any salt within the solution solution. B. in a ternary mixture of 50 mM KCl solution and one of the osmolytes(1.5 M of Glycine, TMAO and Betaine).

Upon establishing the fact that the force profile between the two plates responds to salt stress and hence can be used as an optimal metric, we proceeded to investigate the possible action of osmolytes on the interaction between two plates. Considering precedent usage of charged surfaces as a proxy for investigating the effect of cosolutes on aggregation, we wanted to explore if our present computer model can predict possible effect of osmolytes on inter-plate interaction. In figure 4A, we compare the force profile of two parallel plates in aqueous solution of 1.5 M betaine (green curve), a well-known zwitterionic osmolyte, with that in

neat water (blue curve) and in salt solution (red curve). The concomitant increase in the extent of inter-plate repulsion in a betaine solution (relative to neat water) is evident from the force profiles. These observations clearly suggest that while salt solution would bring the two plates closer, osmolytes would keep the two negatively charged surface mutually far off. The observation was found to be robust across different pH of silica surface (pH 8.0, degree of ionization was 16.6 %) and this is represented in figure S3 (simulation system details at pH 8.0 is represented in figure S2).

These isolated observations on individual salt solution and osmolyte solution prompted us to explore how the two plates would combinatorially respond in a ternary mixture of salt, osmolytes and water. Towards this end, we simulated how the inter-plate force profile in a salt solution would change upon introduction of osmolytes in the same solution. Figure 4B compares the inter-plate force profiles in 0.5 M KCl solution with that in a ternary aqueous mixture of 0.5 M KCl and three different osmolytes, namely 0.5 M KCl + 1.5 M glycine, 0.5 M KCl + 1.5 M TMAO and 0.5 M KCl + 1.5 M betaine. Very interestingly, our simulation predicts that the value of inter-plate force in salt solution significantly increases upon incorporation of any of the three osmolytes. However, the extent of increase in inter-plate force depends on the chemical identity of osmolyte with the magnitude of repulsion decreasing in the order: Betaine > TMAO > glycine. In addition, we have examined the effect of gradually increasing osmolyte concentration in a ternary mixture of salt and osmolyte. As shown in figure S1 B, the addition of higher betaine concentration (1-3 M range) monotonically increases the repulsive force. Together these observation clearly indicates that osmolytes resurrect the native electrostatic interaction between two surfaces which was impaired via salt-screening. The resurrection of native interactions by osmolytes in excess salt condition is reminiscent of a common biological scenario: when the salt stress negatively influences different cellular activities and brings about multiple defective biological functions,[1,2,4,43] cell inherently produces large variety of osmolytes to counteract these toxic cellular changes.

The current observation from our simulation is consistent with previous AFM-based

experiments on a pair of silica surface by Govrin et al,[14] with signature of very similar traits in the salt/osmolyte/water ternary mixture in both cases. In particular, the experimental investigations had provided evidence of resurrection of interaction between a pair of silica surfaces by a larger set of osmolytes including the three investigated in the current modelling efforts. In fact, our results also qualitatively reproduce the previous experimental report on relative order of osmolyte's effect on the force between the two plates modelled at same pH. However, as we would find in the forthcoming paragraphs, a close molecular-level analysis of our all-atom simulation trajectories would posit that the general mechanism hypothesised in the aforementioned experiment does not hold across all osmolytes. In particular, contrary to the hypothesis of osmolyte-induced cation desorption as proposed by previous experiments, our model identifies two independent, osmolyte-specific mechanisms modulating the inter-plate interaction and validates them via complementary experiments.

Dual and mutually exclusive mechanism of osmolytic action.

The density profiles of the constituent ions of KCl salt solution indicated (figure 5A) that cations (K^+) adsorb next to the silica surface and screen the electrostatic charges, while the anions move away to bulk. Accordingly, we focussed our investigation on the interaction of cations with the plates and especially how it get modulated in presence of osmolytes. To understand the microscopic details of the mechanism performed by osmolytes to counteract salt-stress, we have calculated density profile (figure 5B) and preferential binding co-efficient (figure 5C) of cation (here K^+ ion) to estimate how the cations, interact with the silica plates relative to the solvent (water here). The density and preferential binding co-efficient of the cation, computed at a given inter-plate separation (1.6 and 1.8 nm) were compared across ternary solution of water/salt/osmolytes and binary salt solution. Density calculation of cation in figure 5B shows that the cationic density gets decreased in 1.5M glycine solution compared to the 50mM KCl solution (without any osmolyte). But density of cation is not found to be lowered for the other two osmolytes 1.5M TMAO and betaine in 50mM KCl

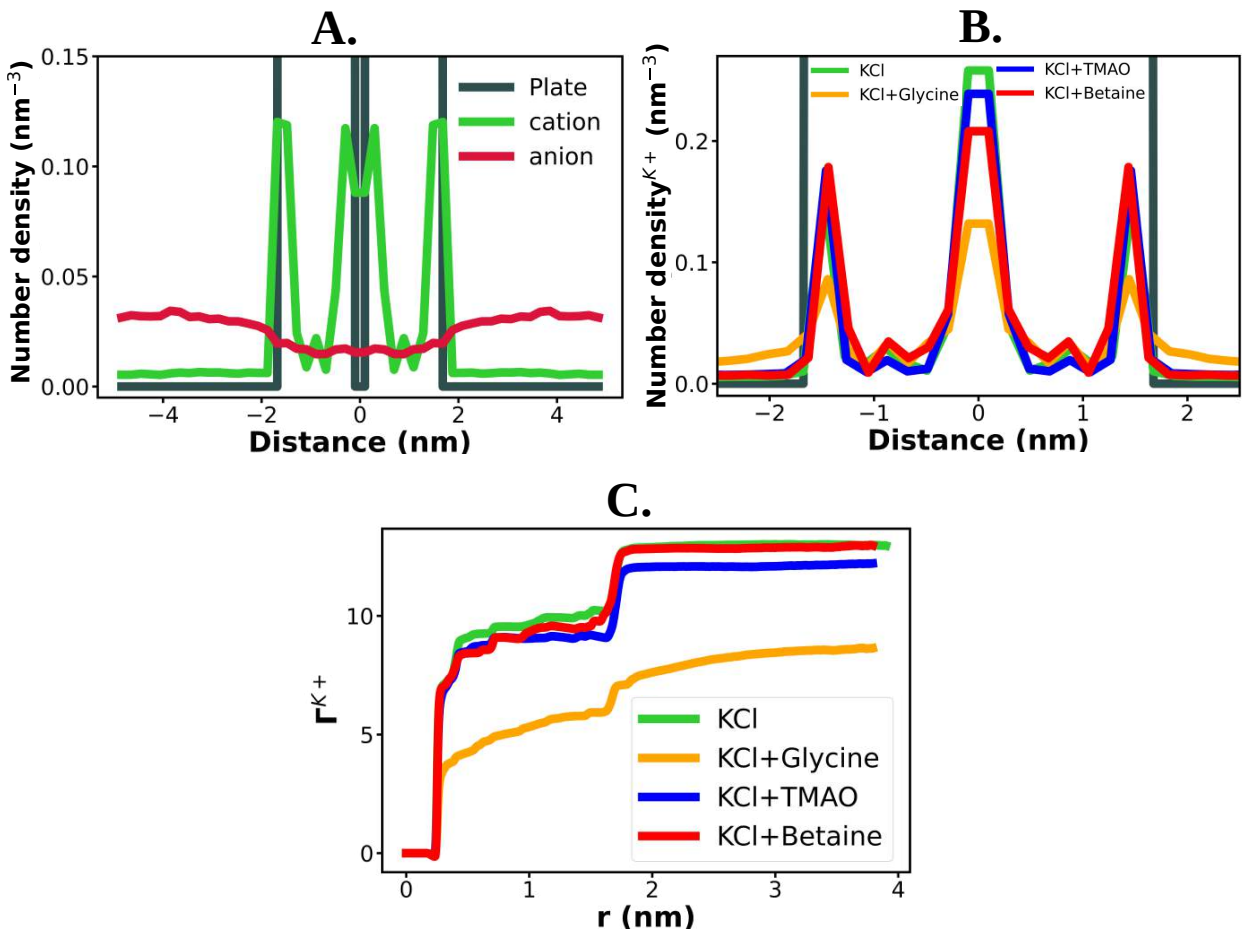

Figure 5: A. the density profiles of cations and anions around silica plates in 50 mM KCl solutions B. shows the density profile of K^+ ions around the silica plates in 50 mM KCl and 1.5 M glycine, TMAO and betaine in 50 mM KCl solution. The plates are shown in grey color in the figure. C. the Preferential binding co-efficient of K^+ (Γ^{K+}) relative to water with respect to the plates in 50 mM aqueous KCl and a ternary mixture of 50 mM KCl in one of the osmolytes (1.5 M Glycine, TMAO and Betaine).

solution. Figure 5C depicts the distance profile of preferential binding coefficient of K^+ ions in absence and in presence of all the three osmolytes individually. The preferential binding coefficient of K^+ (Γ^{K+}) with respect to water reveals that while the value of Γ^{K+} remains unchanged upon incorporation of either betaine (red curve) or TMAO (blue curve) in 50 mM KCl solution(green curve), it gets significantly reduced in presence of glycine in solution (golden yellow curve). This osmolyte-dependent trend indicates that while the direct, preferential adsorption of the cation on the negatively charged plate would remain unperturbed upon addition of betaine or TMAO in a salt solution, the cation will be desorbed from the plate surface in presence of identical concentration of glycine.

The representative simulation snapshots (figure 6) obtained from the MD trajectories of all the three osmolytes (1.5 M glycine, TMAO and betaine in 50 mM KCl solution at pH 5.6) support the aforementioned analysis that, although all three osmolytes are counteracting the salt effect and increases the force among the plates, their underlying mechanism of action are not identical. Visual inspection of the respective snapshots indicated that in presence of glycine, most of the cations remains in the bulk solution rather than being adsorbed on the negatively charged plate surface (figure 6A). On the other hand, for TMAO and betaine (figure 6B and 6C), almost all the cations get adsorbed to the silica surface, with very less in bulk. The relative trends of radial distribution function (g(r)) of cations with the silica surface (figure 6D) are consistent with the visual pictures supporting the fact that the extent of interaction of cations with the silica surface is significantly reduced in presence of glycine in the solution but not by other two osmolytes (betaine and TMAO).

Comparison of the snapshots with respect to the extent of osmolytic interaction with the plates suggests that glycine interacts more strongly with the plates in comparison to the other osmolytes TMAO and betaine. One can observe dense glycine patch around the silica plates, whereas the density of TMAO and betaine near the plate is found to be significantly lesser compared to glycine. These diverse interactions of osmolytes with silica surface could be further verified by estimation of pair correlation function of osmolytes with respect to

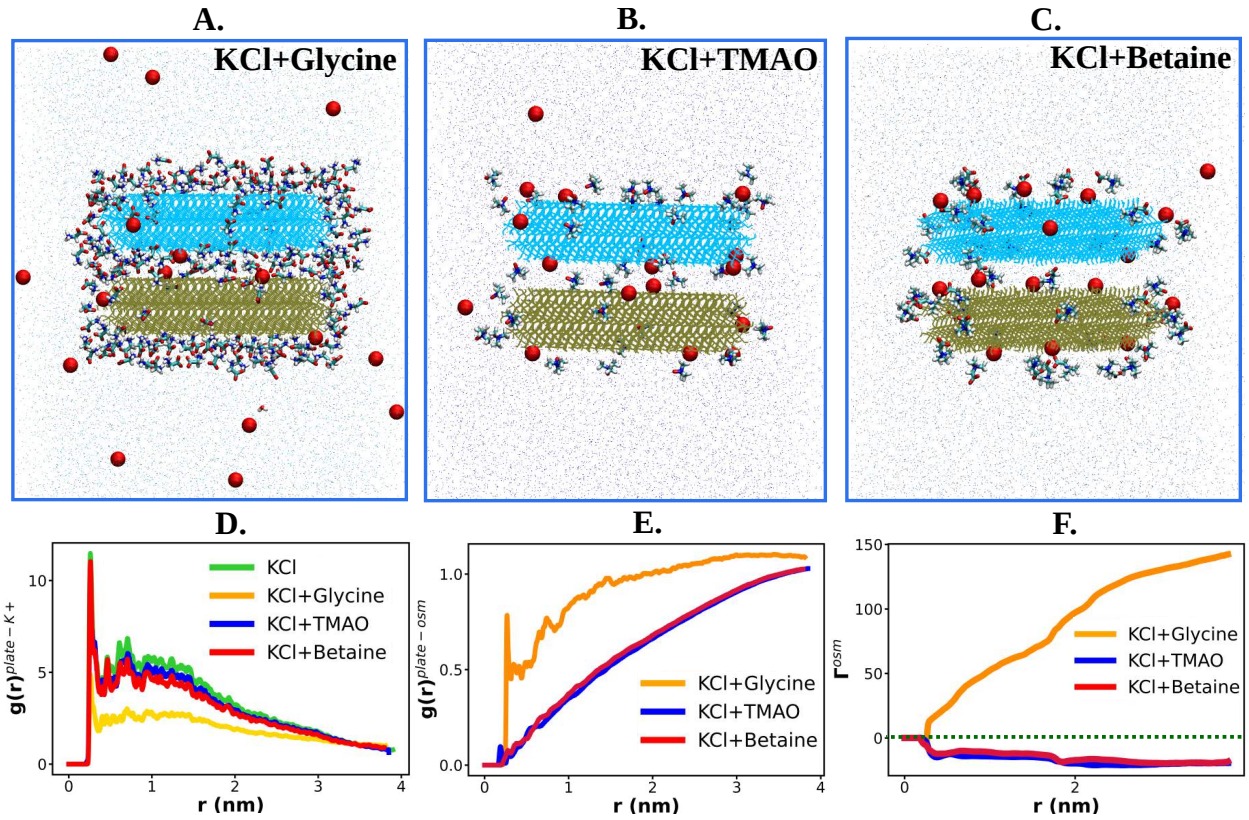

Figure 6: Snapshots in presence of 1.5M A. glycine, B. TMAO and C. betaine. the plates are represented by lines of cyan and olive green color, osmolyte molecules are shown in licorice representation and the K^+ ions are represented by red colored spheres. Figure D. is showing pair correlation function of K+ ions ($g(r)^{plate-K+}$) in 50 mM KCl and 1.5M glycine,TMAO and betaine solution within 50 mM KCl at pH 5.6. In figure E. pair correlation function of the three osmolytes ($g(r)^{plate-osm}$) with respect to plates are shown and figure F. indicates preferential binding co-efficient (Γ_{osm}) of the three osmolytes relative to water with respect to plates (green colored dotted line is indicating the zero value of Γ_{osm}).

plates. The plot indicates (figure 6E) that only glycine would experience strong interaction towards plate surface, whereas TMAO and Betaine do not prefer to interact much with the plates.

For a quantitative characterization of osmolytic interaction with the surfaces, we computed the preferential binding co-efficient of individual osmolytes (Γ^{osm}) (relative to water molecules) with the plates. We find (figure 6F) that, among all three osmolytes, the preferential binding co-efficient is positive only for glycine (above the dotted line) i.e. only glycine will be preferentially adsorbed (with respect to water in the medium) to the plate surface via its direct interaction with the plates. However, for both TMAO and betaine Γ^{osm} are negative (below the dotted line) in its sign which suggests that both TMAO and betaine would get preferentially excluded from silica plates i.e. these two osmolytes generally prefer to be away from the plate surface. Both of these calculations of pair correlation function (figure 6E) and preferential binding co-efficient (figure 6F) together confirm that glycine has the strongest interaction with the plates whereas TMAO and betaine display very weak interaction with the plate, as indicated by significantly less intense peak for both TMAO and betaine. Together all evidences obtained from our model point to dual mechanism of osmolytic interactions that are at play here to counteract salt-stress with varied osmolytic efficiency.

Contact angle measurement and Raman spectroscopy Substantiate simulation result

We employed a set of experiments to validate the simulation-based predictions of contrasting interaction of osmolytes near charged surface. Towards this end, we first performed room temperature contact angle measurements (sessile drop method) for each of the ternary mixtures (glycine, TMAO, and betaine in 50 mM KCl in acetate buffer (pH 5.6) on silicon (Si) wafer having a native oxide layer on its surface. Contact angle provides the quantification of a liquid's ability to wet a solid surface. For the set of systems containing each of the ternary

mixtures surrounding the particular surface (silica here), alteration in the value of contact angle would mostly be driven by the variation in the nature of the liquid interfacing with the solid surface (medium above the free surface of the liquid is also kept unchanged here). The surface tension of the solution acts as the determining factor towards contact angle, which in particular depends on the constituents of solution. The lower the wettability of a surface, the higher will be the corresponding contact angle or the surface tension. With the rise in contact angle, the surface tends to become more hydrophobic. In other words, higher value of contact angle indicates that, in competition between water and other co-solutes to closely interact with solid surface, co-solute would preferentially interacts with the surface, with water receding from the surface. As a result, the contact angle measurement can serve as a very good validation of preferential interaction based analysis obtained in simulation.

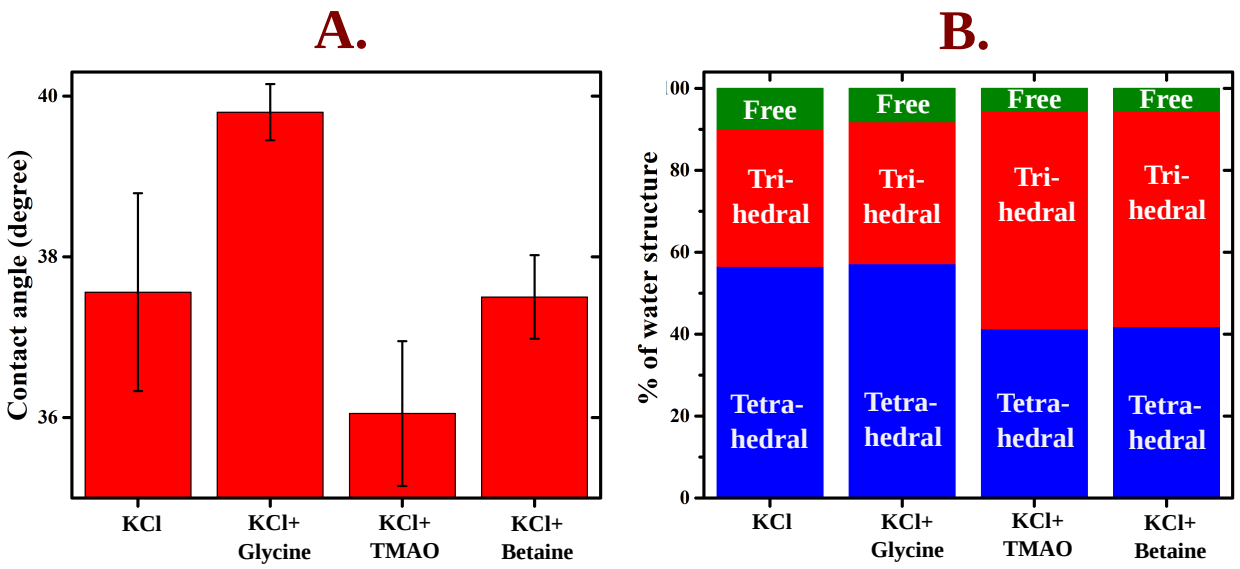

Figure 7: A. The room temperature contact angles (sessile drop) of the three osmolytes (glycine, TMAO and betaine) of 1.5 M concentrations in 50 mM KCl solution on SiO_2 wafer (silicon wafer having native oxide layer and comapred with 50 mM KCl solution. B. This figure represents Raman spectral analysis and a systematic comparison for the 50 mM KCl, 1.5 M Glycine, TMAO and Betaine in 50 mM KCl solution. This figure represents bar plot percentage of water structure respectively for the four systems. Percentage of tetrahedral, trihedral and free water structures are represented in blue, red and green colors respectively.

The contact angle (see figure 7A) of 50 mM KCl in acetate buffer (pH 5.6, control) was measured to be 37.5±1.2°. This was found to be increased to 39.8±0.3° when 1.5M

glycine was introduced to the acetate buffer containing KCl. This also indicates an increase in the surface tension with glycine addition, as observed by others,[44] and it can be due to the modification of silica water interface with glycine adsorption. On the other hand, when the osmolyte is changed from 1.5M glycine to 1.5M TMAO or 1.5M betaine, the contact angle was found to be almost unchanged relative to 50 mM KCl in acetate buffer (36±0.9° and 37.5±0.5° for 1.5M TMAO and 1.5M betaine in acetate buffer containing 50 mM KCl, respectively) indicating a stark contrast from the interface of glycine-silica. The higher contact angle in saline solution containing glycine compared to TMAO and betaine represents lesser hydrophilicity of the surface in glycine solution, whereas for TMAO or betaine there was no such change in surface-hydrophilicity. The lower hydrophilicity of the surface in presence of glycine could be correlated with the strong interaction of glycine to the silica surface which is responsible for lowering the affinity of water and also salt cations with the surface of silica. Thus the rise in contact angle in 1.5M glycine indicates its preferential interaction with plate at the expense of removal of water (making plate more hydrophobic) and salt cations from the plate surface. On the other hand, for TMAO and betaine, the contact angle of ternary solution appeared to be almost similar to that without the presence of osmolytes in solution, suggesting that there is no preferential interaction of these two osmolyte to the plate, relative to water, which could have altered surface hydrophilicity or cationic interaction with the plate. Together, these contact angle measurements lend useful credence to prediction of contrasting preferential interactions of osmolytes from simulation.

Furthermore, the silica-water contact angles are measured with increased osmolyte concentration of 3M (see figure S4) and we have noticed increase in contact angle for each of them with the rise in respective concentration[45] (from 1.5M to 3M). But the contact angle increment for glycine (39.8±0.3° to 53±1.3°) is found to be much higher than that in TMAO (36±0.9° to 44±2.5°) and betaine (37.5±0.5° to 46.3±1.1°). This again confirms that glycine-silica interaction is significantly higher than that of TMAO or betaine with SiO_2 (silica) leading to desorption of cations from the silica surface in presence of glycine.

To further look in to the structure of silica-water interface with different osmolytes, we have performed surface enhanced Raman spectroscopy (SERS). Since the discovery in 1970s,[46,47] SERS is being widely used in various applications like medicinal chemistry, material science, electrochemistry, analytical chemistry and catalysis.[48–51] Ultra-high sensitivity of SERS can give single molecular information compared to other spectroscopic technique like single-molecule fluorescence spectroscopy.[52–54] But the use of roughen surfaces of only Au, Cu and Ag bottle-necks in the general applicability of SERS. First breakthrough was the discovery of tip enhanced Raman spectroscopy (TERS) for the general application of SERS independent of any surfaces and substrates.[55] Here we have employed another general technique of SERS i.e. shell-isolated nanoparticle enhanced micro-Raman spectroscopy (SHINERS) to perform SERS of smooth SiO_2 substrate to investigate the SiO_2-osmolyte interaction. shell-isolated nanoparticle enhanced micro-Raman spectroscopy (SHINERS).

SHINERS is a powerful technique to find the Raman modes of the molecules (here water and SiO_2) placed near the solid interface (silica). The details of the experiment are given in the method section and the schematic of SHINERS experiment setup is shown in figure 3. In a nutshell, gold nanoparticle (55 nm) core -silica (5 nm) shell nanoparticles ($Au@SiO_2$ np) were synthesized using a previously reported method[41] and drop casted over a clean silicon surface for SHINERS studies. SHINERS is performed to investigate the effect of osmolytes on SiO_2 Raman vibration mode at 520 cm^{-1}. Any interaction between osmolyte and SiO_2 will be reflected in the SiO_2 Raman vibration mode. But it is clear from figure S5 A that the SiO_2 mode is not getting affected with the addition of different osmolytes of same concentration (1.5M).[56] But changes in the H-OH stretching of water at 2800-3800 cm^{-1} was observed, (shown in figure S5 B).[57,58]

Bulk water consists of different water structures depending on the degree of hydrogen bonding present. Here, the broad water stretching peak can be deconvoluted into three gaussian peaks (figure S6) to calculate the percentage of water present in that structure namely: tetrahedrally coordinated water (four H-bonding/water molecule, 3200 cm^{-1}), trihedrally

coordinated water (liquid like, three H-bonding/water molecule, 3400 cm^{-1}), and free water (no H-bonding, 3600 cm^{-1}). More percentage of water present in tetrahedral form signifies that water is more ordered. Lesser interaction with other surfaces like SiO_2 would mean increased concentration of tetrahedrally coordinated water structure. The concentration of tetrahedrally coordinated water present in 50 mM KCl in acetate buffer of pH 5.6 is 56%, (figure 7B). However, after adding 1.5 M glycine to the salt solution, the tetrahedral water concentration increases to 57% while the percentage of tetrahedral water decreases to 41% in 1.5 M TMAO. Tetrahedral water amount of 41% is found in 1.5 M betaine. The trend suggests that after adding 1.5M glycine to the 50 mM KCl in acetate buffer, the hydrogen-bonding network of water in acetate buffer at the interface is getting extended because of the strong glycine- SiO_2 interaction, forcing water away from the Silica surface in tune with the increased contact angle. Due to lesser interaction between TMAO or betaine with SiO_2, most of the betaine or TMAO remains in the bulk acetate buffer away from SiO_2 surface, breaking its Hydrogen-bonding network which is reflected in less amount of tetrahedral water coordination.

Together the contact angle measurement and spectral analysis support our computational prediction of contrasting preferential interactions of the osmolytes and confirm the prevalence of dual mechanisms for resurrection of charges in salt solution.

Dissecting Molecular origin of osmolyte's dual mechanism

The precedent joint simulation/experiment ventures have indicated the interplay of two independent, osmolyte-specific mechanisms, via which salt-screening of negatively charged surfaces can be counter-acted via a set of osmolytes : Glycine would competitively desorb the cations from the silica interfaces and itself would preferentially interact with the surfaces. On the other hand, betaine and TMAO would not alter the cation density in-between and around the plate; Rather these osmolytes would also have significantly much lesser propensity of interaction with the plate than glycine.

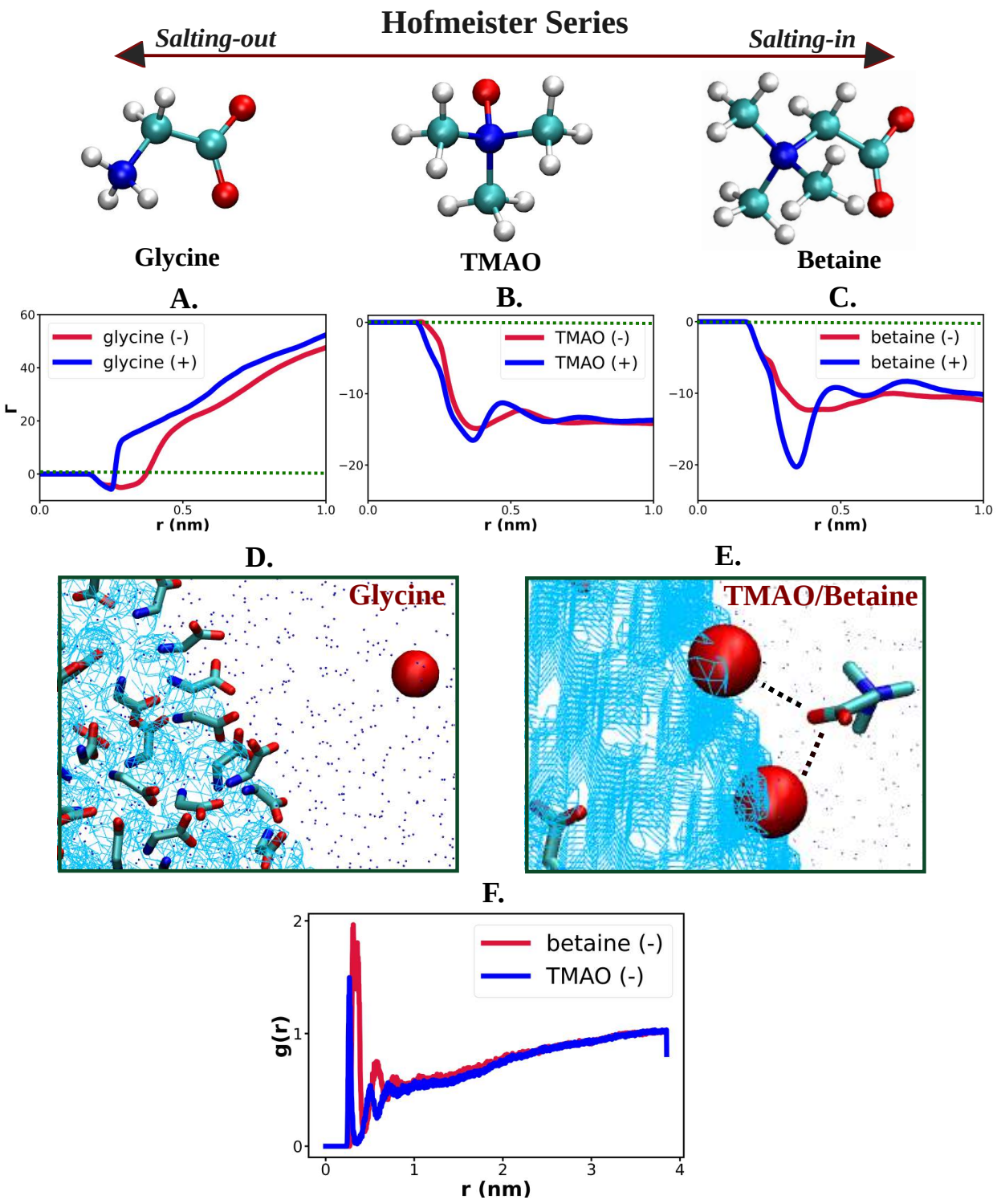

Figure 8: Preferential binding co-efficient of both negatively (red) and positively (blue) charged moieties of zwitter-ionic osmolytes are represented for 1.5 M A. glycine, B. TMAO and C. betaine in 50 mM KCl solution. Figure D and E. represent the snapshots showing interaction of cation and osmolytes with the plates for glycine and betaine respectively. Silica plates are fabricated with cyan colored lines and the cations are in red sphere representation and osmolytes are shown in licorice form with red colored anionic moieties and cationic moieties in blue color. Figure F. shows the pair correlation function of anioninc part of TMAO (blue) and betaine (red) from the cation adsorbed silica surface.

In seeking to elucidate the molecular origin behind this ambivalent mechanism, we dissect the relative interaction of different functional moieties of the osmolytes with the interface as well as with ions. For a more focussed analysis, we individually computed Γ^{osm} of positive and negative part of each osmolytes. (figure 8A-C) We find that for glycine, the preferential binding coefficient is higher (more positive) for positively polar end of the molecule (figure 8A), suggesting that the glycine is majorly interacting with the plate via its amine site rather the negative part of glycine. On the other hand, while TMAO and betaine would prefer to remain excluded from the silica interface, the extent of exclusion will be relatively lesser for the anionic carboxylate part than the cationic amine part, as ascertained by the respective trend of Γ^{osm} of TMAO and betaine (figure 8B-C).

We believe that the observed contrast between the mechanism of interaction of glycine and TMAO/Betaine arises due to the presence of methyl group (betaine/TMAO) attached to the positively charged nitrogen atom or lack thereof (glycine) (see figure 1). The presence of methyl groups at nitrogen atom bearing positive charge, serves two roles : 1) the electron pushing inductive effect of three methyl groups effectively reduces the positive charge density of the zwitter-ion. Hence both the TMAO and betaine would have lesser tendency to interact with the negatively charged plates compared to glycine (confirmed by Γ^{osm} in figure 8A-C) 2) the presence of three bulky methyl groups in TMAO and betaine would sterically hinder them from interacting with the plates. Together, these two factors would contribute to direct and more efficient electrostatic interaction of glycine with negatively charged plates via its amine functional group, as opposed to significantly weaker interaction between plate and other two osmolytes.

The preferential adsorption of glycine molecules near the silica surface (figure 8A see positive Γ^{osm}) due to the aforementioned reasons would electronically and sterically keep the cations (K^+ ions) away from the plates, resulting in relatively enhanced inter-plate repulsions than that in osmolyte-free saline water.(see figure 8D for a representative snapshot.) On the contrary, the electrostatic attractions between the adsorbed cations and the nega-

tively polar end of these TMAO and betaine (see g(r) between cation and osmolytes figure 8F) would retain the cations adsorbed near the silica surface, essentially creating a cation-mediated interactions between the plates and negative polar end of the of the osmolyte (see a representative snapshot in figure 8E). The favorable interaction between the cation and the negative pole of the osmolyte will also neutralize the ion's charge-screening ability, leading to enhanced inter-plate repulsion.

In summary, not all the osmolytes would adopt similar mechanism to fight against osmotic stress, as suggested by previous investigations.[14] The osmolyte glycine, which directly interact with the surface would competitively desorb cations responsible for charge-screening. In contrast, the other osmolytes TMAO and betaine which can not displace the cations from the surface, would circumvent the cation's charge-screening via partial neutralization of the adsorbed cations.

Justifying Hofsmeister series for the osmolytes.

Here we seek a justification for the relative efficiency of resurrection of inter-plate electrostatic repulsion which follows the order Glycine $<$ TMAO $<$ Betaine at pH 5.6 (see figure 4B and the Hofmeister series represented in figure 8). All the osmolytes attempt to minimise cation's screening effect by modulating the charge density of the adsorbed cations, but the comparative osmolytic efficiency is driven by their relative interaction with plates and cations. Though glycine desorbs cations and attempts to resurrect inter-plate force, but unlike TMAO and betaine, glycine's direct interaction with silica does not allow it to restore the force to similar extent. While presence of glycine near the surface desorbs the cations but also partially neutralizes the surface charge (negative) of silica plates via its positively polar amine group. Thus these two contrasting effects of surface charge screening by glycine are responsible for lowering glycine's effectivity in inter-plate force resurrection. On the other hand, this aforementioned opposing effect of partial surface charge neutralization through direct osmolytic interaction does not come to play for TMAO and betaine. The presence of

bulky methyl groups attached to the positively charged trimethyl amine does not electronically and sterically allow TMAO or betaine to preferentially interact with the silica plates. Thus unlike glycine, TMAO and betaine would not reduce the surface charge density of silica plates through the positively charged functional group of the osmolytes. Rather it would more efficiently resurrect force than glycine via neutralising the charge density of cations adsorbed to the negatively charged surface. Finally among TMAO and betaine, the later is found to act more efficiently in restoring the repulsion between two silica plates. Both of these two osmolytes counteract the screening effect of salt-cations by partially neutralizing cationic charge density through the negatively charged moiety of the zwitter-ionic structure. Comparing the extent of cation neutralization by the anionic part of the osmolytes, we have observed that betaine is interacting relatively more strongly (offering more effective partial charge density neutralization of catinos) with the adsorbed cations (K^+ ions) than TMAO and this would make betaine more skilled in combating salt-stress. Therefore betaine acts most efficiently against salt stress follwed by TMAO and then glycine.

Conclusion

The mechanism responsible for osmolyte action in adjusting osmotic balance within the cell is a longstanding question. The high concentration tolerance of osmolytes in biology, their diverse important roles to perform as life saver for a wide range of organisms has raised profound interest about it. Along with other osmotic stress factor, salinity stress stands as one of the most detrimental factors to induce osmotic shock. While the osmoprotective roles of small molecules have been explored for decade, the mechanistic details of their performance in relieving saline stress to preserve proper physiological function of cells still remains as a grey area. Especially the role of these neutral cosolutes in modulating electrostatic interactions, as opposed to noncoloumic interactions, has eluded detailed investigations, until recently. Recent investigations[3,13,14] have explored the role of osmolytes in counteracting

salt-stress and cited electrostatic interaction as the major contribution by the osmolytes to combat osmotic stress originated due to cellular electrolytic imbalance. These precedent investigations had inspired us to look into the osmolytic performance in maintaining suitable cellular osmotic balance at an atomic resolution and evaluate the underlying mechanisms via atomically precise computer simulation. Here we have assembled a collaborative effort of molecular dynamics simulation and interfacial experiments to elucidate the role of the combination of salt and multiple osmolytes to overcome the adverse salt-effect faced by a pair of negatively charged surfaces.

While our computer models reproducibly recapitulate previously reported the osmolyte-mediated resurrection of electrostatic forces,[14] which had been hitertho screened by salts, our investigations offer differing viewpoints on the concomitant role of the osmolytes. Contrary to prevalent hypothesis that restoration of force among the plates occurs only by competitive desorption of adsorbed cations by all the osmolytes, we report a dual and mutually contrasting mechanisms which are specific to the chemical nature of the osmolytes. Via a detailed analysis of mechanism of action three osmolytes (glycine, TMAO and betaine) for combating salt-stress, our joint theory/experiment investigations establish that only for glycine, desorption of cations takes place from the plate surface due to the direct interaction of glycine with the plates via its electrostatically favoured positive amine functional group. On the other hand for other two osmolytes, in fact, no such cation desorption happens. Analysis of simulation trajectories indicate that partial neutralization of charge density of adsorbed cations by TMAO and betaine acts as the key factor for opposing the salt driven screening effect. This partial neutralization of cationic charge density by interaction of the negatively charged moiety of osmolytes makes the adsorbed cations less efficient to screen the surface charges. Thus according to our results, unlike glycine, TMAO and betaine resurrects the repulsion among the plates mostly by neutralization of adsorbed cation, instead of removing those from the surface. Contact angle measurements and Raman spectroscopy based analysis of interfacial water aptly corroborate the predictions of the osmolyte-specific

mechanism of the simulation. The simulation models also correctly captures and interprets the relative trend of efficiency for resurrection of force by the osmolytes.

Since a large part of the cellular macromolecules are negatively charged, easy and instantaneous cation adsorption to the biomolecular surfaces decreases its tendency to remain solubilized (due to protein aggregation) and make it prone towards misfolding by weakening inter and intra protein repulsion under salt stress. Recent publication has shown the effect of osmolytes on protein dimerization[3] and conformation[59,60] of biomolecules. Osmolytes restore protein repulsion following diverse mechanisms mostly based on Coulombic interactions (with salt and biomolecular surface) and thus maintains required protein-protein interaction and enzyme-substrate recognition for proper functioning of cell. We believe the access to the dual and mutually contrasting modes of osmolyte interactions, as has been elucidated by our investigations, would help the biological cell to be more adaptable with the surroundings and would provide it the required biological flexibility to cope up to the adverse changes of nature. In future it will be beneficial to explore how different osmolyte behave in different temperatures and thus can protect cells with external extreme conditions and different pH.

Supplemental Information

All supplemental figures described in the article (PDF)

Acknowledgements

This work was supported by computing resources obtained from shared facility of TIFR Centre for Interdisciplinary Sciences, India. We acknowledge support of the Department of Atomic Energy, Government of India, under Project Identification No. RTI 4007. JM acknowledges Core Research grants provided by the Department of Science and Technology (DST) of India (CRG/2019/001219).

References

(1) Attri, P.; Venkatesu, P.; Lee, M.-J. Influence of Osmolytes and Denaturants on the Structure and Enzyme Activity of alpha-Chymotrypsin. *The Journal of Physical Chemistry B* **2010**, *114*, 1471–1478.

(2) Huang, Y.; Bie, Z.; Liu, Z.; Zhen, A.; Wang, W. Protective role of proline against salt stress is partially related to the improvement of water status and peroxidase enzyme activity in cucumber. *Soil Science and Plant Nutrition* **2009**, *55*, 698–704.

(3) Rydeen, A. E.; Brustad, E. M.; Pielak, G. J. Osmolytes and Protein-Protein Interactions. *Journal of the American Chemical Society* **2018**, *140*, 7441–7444, PMID: 29842777.

(4) Brocker, C.; Thompson, D. C.; Vasiliou, V. The role of hyperosmotic stress in inflammation and disease. *BioMolecular Concepts* **2012**, *3*, 345–364.

(5) Greenway, H.; Osmond, C. B. Salt Responses of Enzymes from Species Differing in Salt Tolerance. *Plant Physiology* **1972**, *49*, 256–259.

(6) Munns, R.; Tester, M. Mechanisms of Salinity Tolerance. *Annual Review of Plant Biology* **2008**, *59*, 651–681.

(7) Ashraf, M.; Foolad, M. Roles of glycine betaine and proline in improving plant abiotic stress resistance. *Environmental and Experimental Botany* **2007**, *59*, 206–216.

(8) Knowles, D. B.; Shkel, I. A.; Phan, N. M.; Sternke, M.; Lingeman, E.; Cheng, X.; Cheng, L.; O'Connor, K.; Record, M. T. Chemical Interactions of Polyethylene Glycols (PEGs) and Glycerol with Protein Functional Groups: Applications to Effects of PEG and Glycerol on Protein Processes. *Biochemistry* **2015**, *54*, 3528–3542.

(9) Guinn, E. J.; Pegram, L. M.; Capp, M. W.; Pollock, M. N.; Record, M. T. Quantify-

ing why urea is a protein denaturant, whereas glycine betaine is a protein stabilizer. *Proceedings of the National Academy of Sciences* **2011**, *108*, 16932–16937.

(10) Xie, G.; Timasheff, S. N. Mechanism of the stabilization of ribonuclease a by sorbitol: Preferential hydration is greater for the denatured than for the native protein. *Protein Science* **1997**, *6*, 211–221.

(11) Zhang, Y.; Cremer, P. S. Chemistry of Hofmeister Anions and Osmolytes. *Annual Review of Physical Chemistry* **2010**, *61*, 63–83.

(12) Liao, Y.-T.; Manson, A. C.; DeLyser, M. R.; Noid, W. G.; Cremer, P. S. TrimethylamineN-oxide stabilizes proteins via a distinct mechanism compared with betaine and glycine. *Proceedings of the National Academy of Sciences* **2017**, *114*, 2479–2484.

(13) Liao, Y.-T.; Manson, A. C.; DeLyser, M. R.; Noid, W. G.; Cremer, P. S. TrimethylamineN-oxide stabilizes proteins via a distinct mechanism compared with betaine and glycine. *Proceedings of the National Academy of Sciences* **2017**, *114*, 2479–2484.

(14) Govrin, R.; Tcherner, S.; Obstbaum, T.; Sivan, U. Zwitterionic Osmolytes Resurrect Electrostatic Interactions Screened by Salt. *Journal of the American Chemical Society* **2018**, *140*, 14206–14210.

(15) Govrin, R.; Schlesinger, I.; Tcherner, S.; Sivan, U. Regulation of Surface Charge by Biological Osmolytes. *Journal of the American Chemical Society* **2017**, *139*, 15013–15021.

(16) Govrin, R.; Obstbaum, T.; Sivan, U. Common Source of Cryoprotection and Osmoprotection by Osmolytes. *Journal of the American Chemical Society* **2019**, *141*, 13311–13314.

(17) Choi, Y. K.; Kern, N. R.; Kim, S.; Kanhaiya, K.; Afshar, Y.; Jeon, S. H.; Jo, S.; Brooks, B. R.; Lee, J.; Tadmor, E. B.; Heinz, H.; Im, W. CHARMM-GUI Nanomaterial Modeler for Modeling and Simulation of Nanomaterial Systems. *Journal of Chemical Theory and Computation* **2022**, *18*, 479–493.

(18) Jo, S.; Kim, T.; Iyer, V. G.; Im, W. CHARMM-GUI: A web-based graphical user interface for CHARMM. *J. Comput. Chem.* **2008**, *29*, 1859–1865.

(19) Emami, F. S.; Puddu, V.; Berry, R. J.; Varshney, V.; Patwardhan, S. V.; Perry, C. C.; Heinz, H. Force Field and a Surface Model Database for Silica to Simulate Interfacial Properties in Atomic Resolution. *Chemistry of Materials* **2014**, *26*, 2647–2658.

(20) Heinz, H.; Lin, T.-J.; Mishra, R. K.; Emami, F. S. Thermodynamically Consistent Force Fields for the Assembly of Inorganic, Organic, and Biological Nanostructures: The INTERFACE Force Field. *Langmuir* **2013**, *29*, 1754–1765.

(21) Lin, T.-J.; Heinz, H. Accurate Force Field Parameters and pH Resolved Surface Models for Hydroxyapatite to Understand Structure, Mechanics, Hydration, and Biological Interfaces. *The Journal of Physical Chemistry C* **2016**, *120*, 4975–4992.

(22) Heinz, H.; Vaia, R. A.; Farmer, B. L.; Naik, R. R. Accurate Simulation of Surfaces and Interfaces of Face-Centered Cubic Metals Using 12-6 and 9-6 Lennard-Jones Potentials. *The Journal of Physical Chemistry C* **2008**, *112*, 17281–17290.

(23) Hart, K.; Foloppe, N.; Baker, C. M.; Denning, E. J.; Nilsson, L.; MacKerell, A. D. Optimization of the CHARMM Additive Force Field for DNA: Improved Treatment of the BI/BII Conformational Equilibrium. *J. Chem. Theory Comput.* **2012**, *8*, 348–362.

(24) Mukherjee, M.; Mondal, J. Unifying the Contrasting Mechanisms of Protein-Stabilizing Osmolytes. *The Journal of Physical Chemistry B* **2020**, *124*, 6565–6574.

(25) Ganguly, P.; Hajari, T.; Shea, J.-E.; van der Vegt, N. F. A. Mutual Exclusion of Urea and Trimethylamine N-Oxide from Amino Acids in Mixed Solvent Environment. *The Journal of Physical Chemistry Letters* **2015**, *6*, 581–585.

(26) Larini, L.; Shea, J.-E. Double Resolution Model for Studying TMAO/Water Effective Interactions. *The Journal of Physical Chemistry B* **2013**, *117*, 13268–13277.

(27) Best, R. B.; Zhu, X.; Shim, J.; Lopes, P. E. M.; Mittal, J.; Feig, M.; MacKerell, A. D. Optimization of the Additive CHARMM All-Atom Protein Force Field Targeting Improved Sampling of the Backbone phi, psi and Side-Chain chi1 and chi2 Dihedral Angles. *Journal of Chemical Theory and Computation* **2012**, *8*, 3257–3273.

(28) Kast, K. M.; Brickmann, J.; Kast, S. M.; Berry, R. S. Binary Phases of Aliphatic N-Oxides and Water: Force Field Development and Molecular Dynamics Simulation. *The Journal of Physical Chemistry A* **2003**, *107*, 5342–5351.

(29) Schneck, E.; Horinek, D.; Netz, R. R. Insight into the Molecular Mechanisms of Protein Stabilizing Osmolytes from Global Force-Field Variations. *The Journal of Physical Chemistry B* **2013**, *117*, 8310–8321.

(30) MacKerell, A. D. et al. All-Atom Empirical Potential for Molecular Modeling and Dynamics Studies of Proteins. *J. Phys. Chem. B* **1998**, *102*, 3586–3616, PMID: 24889800.

(31) Bussi, G.; Donadio, D.; Parrinello, M. Canonical sampling through velocity rescaling. *The Journal of Chemical Physics* **2007**, *126*, 014101.

(32) Berendsen, H. J. C.; Postma, J. P. M.; van Gunsteren, W. F.; DiNola, A.; Haak, J. R. Molecular dynamics with coupling to an external bath. *The Journal of Chemical Physics* **1984**, *81*, 3684–3690.

(33) Nosé, S. A molecular dynamics method for simulations in the canonical ensemble. *Mol. Phys.* **1984**, *52*, 255.

(34) Hoover, W. Canonical dynamics: equilibrium phase-space distributions. *Phys. Rev. A* **1985**, *31*, 1695.

(35) Darden, T.; York, D.; Pedersen, L. Particle mesh Ewald: AnN·log(N) method for Ewald sums in large systems. *J. Chem. Phys.* **1993**, *98*, 10089–10092.

(36) Hess, B.; Bekker, H.; Berendsen, H. J. C.; Fraaije, J. G. E. M. LINCS: A linear constraint solver for molecular simulations. *J. Comp. Chem* **1997**, *18*, 1463–1472.

(37) Miyamoto, S.; Kollman, P. A. Settle: An analytical version of the SHAKE and RATTLE algorithm for rigid water models. *J. Comp. Chem* **1992**, *13*, 952–962.

(38) Abraham, M. J.; Murtola, T.; Schulz, R.; Pall, S.; Smith, J. C.; Hess, B.; Lindahl, E. GROMACS: High performance molecular simulations through multi-level parallelism from laptops to supercomputers. *SoftwareX* **2015**, *1-2*, 19 – 25.

(39) Wyman, J. Linked Functions and Reciprocal Effects in Hemoglobin: A Second Look. *Adv. Protein Chem.* **1964**, *19*, 223–286.

(40) Tanford, C. Extension of the theory of linked functions to incorporate the effects of protein hydration. *J. Mol. Biol.* **1969**, *39*, 539–544.

(41) Li, C.; Le, J.; Wang, Y.; Chen, S.; Yang, Z.; Li, J.; Cheng, J.; Tian, Z. In situ probing electrified interfacial water structures at atomically flat surfaces. *Nat. Mater.* **2019**, *18*, 697–701.

(42) Li, J. F.; Tian, X. D.; Li, S. B.; Anema, J. R.; Yang, Z. L.; Ding, Y.; Wu, Y. F.; Zeng, Y. M.; Chen, Q. Z.; Ren, B.; Wang, Z. L.; Tian, Z. Q. Surface analysis using shell-isolated nanoparticle-enhanced Raman spectroscopy. *Nature Protocols* **2012**, *8*, 52–65.

(43) Bortner, C. D.; Scoltock, A. B.; Sifre, M. I.; Cidlowski, J. A. Osmotic Stress Resistance

Imparts Acquired Anti-apoptotic Mechanisms in Lymphocytes. *Journal of Biological Chemistry* **2012**, *287*, 6284–6295.

(44) Rodraguez, D. M.; Romero, C. M. Surface Tension of Glycine, Alanine, Aminobutyric acid, Norvaline and Norleuchine in water and in aqueous solutions of strong electrolytes at temperature from 293.15 to 313.15 K. *J. Chem. Eng. Data* **2017**, *62*, 3687–3696.

(45) N. Sghaier, M. P.; Nasrallah, S. B. On the Influence of sodium chloride concentration on equilibrium contact angle. *Chem. Eng. J.* **2006**, *122*, 47–53.

(46) Albrecht, M. G.; Creighton, J. A. Anomalously intense Raman spectra of pyridine at a silver electrode. *Journal of the American Chemical Society* **1977**, *99*, 5215–5217.

(47) Fleischmann, M.; Hendra, P.; McQuillan, A. Raman spectra of pyridine adsorbed at a silver electrode. *Chemical Physics Letters* **1974**, *26*, 163–166.

(48) Chen, Z.; Tabakman, S. M.; Goodwin, A. P.; Kattah, M. G.; Daranciang, D.; Wang, X.; Zhang, G.; Li, X.; Liu, Z.; Utz, P. J.; Jiang, K.; Fan, S.; Dai, H. Protein microarrays with carbon nanotubes as multicolor Raman labels. *Nature Biotechnology* **2008**, *26*, 1285–1292.

(49) Doering, W. E.; Nie, S. Spectroscopic Tags Using Dye-Embedded Nanoparticles and Surface-Enhanced Raman Scattering. *Analytical Chemistry* **2003**, *75*, 6171–6176.

(50) Qian, X.; Peng, X.-H.; Ansari, D. O.; Yin-Goen, Q.; Chen, G. Z.; Shin, D. M.; Yang, L.; Young, A. N.; Wang, M. D.; Nie, S. In vivo tumor targeting and spectroscopic detection with surface-enhanced Raman nanoparticle tags. *Nature Biotechnology* **2007**, *26*, 83–90.

(51) Cao, Y. C.; Jin, R.; Mirkin, C. A. Nanoparticles with Raman Spectroscopic Fingerprints for DNA and RNA Detection. *Science* **2002**, *297*, 1536–1540.

(52) Nie, S.; Emory, S. R. Probing Single Molecules and Single Nanoparticles by Surface-Enhanced Raman Scattering. *Science* **1997**, *275*, 1102–1106.

(53) Nie, S.; Zare, R. N. OPTICAL DETECTION OF SINGLE MOLECULES. *Annual Review of Biophysics and Biomolecular Structure* **1997**, *26*, 567–596.

(54) Kneipp, K.; Wang, Y.; Kneipp, H.; Perelman, L. T.; Itzkan, I.; Dasari, R. R.; Feld, M. S. Single Molecule Detection Using Surface-Enhanced Raman Scattering (SERS). *Physical Review Letters* **1997**, *78*, 1667–1670.

(55) Stöckle, R. M.; Suh, Y. D.; Deckert, V.; Zenobi, R. Nanoscale chemical analysis by tip-enhanced Raman spectroscopy. *Chemical Physics Letters* **2000**, *318*, 131–136.

(56) Popovic, D. M.; Milosavljevic, V.; Zekic, A.; Romcevic, N.; Daniels, S. Raman scattering analysis of silicon dioxide single crystal treated by direct current plasma discharge. *Appl. Phys. Lett.* **2011**, *98*.

(57) Stefanski,; Johannes,; Schmidt,; Christian,; Jahn,; Sandro, Aqueous sodium hydroxide (NaOH) solutions at high pressure and temperature: insights from in situ Raman spectroscopy and ab initio molecular dynamics simulations. *Phys. Chem. Chem. Phys.* **2018**, *20*, 21629–21639.

(58) Shen, L.; Lu, B.; Li, Y.; Liua, J.; Huangfu, Z.; Peng, H.; Ye, J.; Qu, X.; Zhang, J.; Li, G.; Cai, W.; Jiang, Y.; Sun, S. *Angew. Chemie* **2020**, *132*, 22583–22588.

(59) Mondal, J.; Halverson, D.; Li, I. T. S.; Stirnemann, G.; Walker, G. C.; Berne, B. J. How osmolytes influence hydrophobic polymer conformations: A unified view from experiment and theory. *Proc. Natl. Acad. Sci. USA* **2015**, *112*, 9270–9275.

(60) Mukherjee, M.; Mondal, J. Osmolyte-Induced Macromolecular Aggregation Is Length-Scale Dependent. *The Journal of Physical Chemistry B* **2019**, *123*, 8697–8703, PMID: 31539258.

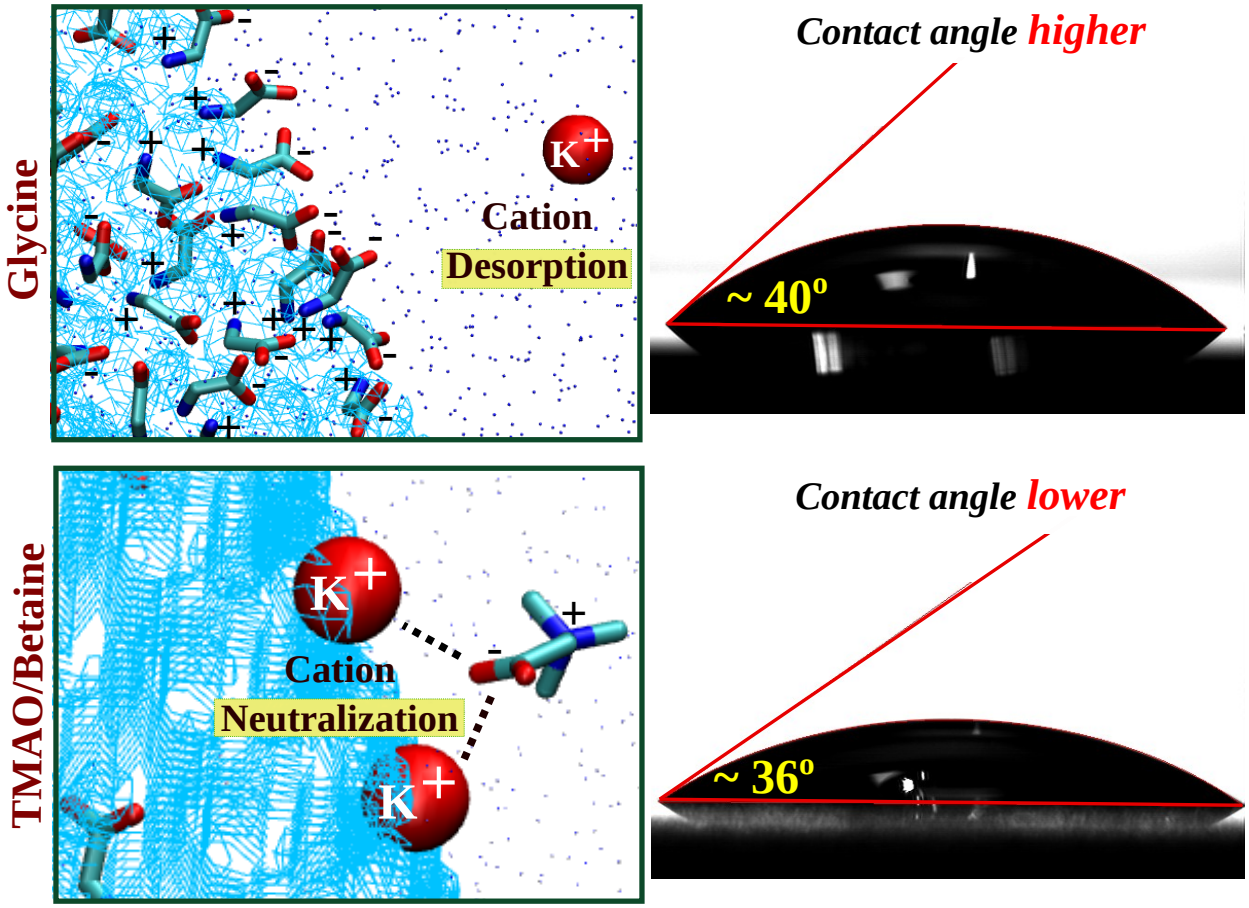

Table of Content